EXEL-7647 Inhibits Mutant Forms of ErbB2 Associated with Lapatinib Resistance and Neoplastic Transformation

Torsten Trowe, Sotiria Boukouvala, Keith Calkins, Richard E. Cutler, Jr., Ryan Fong, Roel Funke, Steven B. Gendreau, Yong D. Kim, Nicole Miller, John R. Woolfrey, Valentina Vysotskaia, Jing Ping Yang, Mary E. Gerritsen, David J. Matthews, Peter Lamb, and Timothy S. Heuer

Abstract

Purpose: Mutations associated with resistance to kinase inhibition are an important mechanism of intrinsic or acquired loss of clinical efficacy for kinase-targeted therapeutics. We report the prospective discovery of ErbB2 mutations that confer resistance to the small-molecule inhibitor lapatinib.

Experimental Design: We did *in vitro* screening using a randomly mutagenized ErbB2 expression library in Ba/F3 cells, which were dependent on ErbB2 activity for survival and growth.

Results: Lapatinib resistance screens identified mutations at 16 different ErbB2 amino acid residues, with 12 mutated amino acids mapping to the kinase domain. Mutations conferring the greatest lapatinib resistance cluster in the NH_2-terminal kinase lobe and hinge region. Structural computer modeling studies suggest that lapatinib resistance is caused by multiple mechanisms; including direct steric interference and restriction of conformational flexibility (the inactive state required for lapatinib binding is energetically unfavorable). ErbB2 T798I imparts the strongest lapatinib resistance effect and is analogous to the epidermal growth factor receptor T790M, ABL T315I, and cKIT T670I gatekeeper mutations that are associated with clinical drug resistance. ErbB2 mutants associated with lapatinib resistance transformed NIH-3T3 cells, including L755S and T733I mutations known to occur in human breast and gastric carcinomas, supporting a direct mechanism for lapatinib resistance in ErbB2-driven human cancers. The epidermal growth factor receptor/ErbB2/vascular endothelial growth factor receptor inhibitor EXEL-7647 was found to inhibit almost all lapatinib resistance-associated mutations. Furthermore, no ErbB2 mutations were found to be associated with EXEL-7647 resistance and lapatinib sensitivity.

Conclusions: Taken together, these data suggest potential target-based mechanisms of resistance to lapatinib and suggest that EXEL-7647 may be able to circumvent these effects.

The discovery of genetic alterations associated with tumor growth and therapeutic response is critical to the development of effective cancer therapeutics. Kinase activation by mutation, gene amplification, or other means can engage growth-regulating signal transduction pathways that play vital roles in many cancers. Discoveries connecting kinase activation with defined types of human cancer (e.g., BCR-ABL with chronic myelogenous leukemia or cKIT with gastrointestinal stromal tumors) have led to the successful use of kinase inhibitors as cancer therapies. However, certain patients fail to respond, and often, favorable patient response to kinase inhibition is followed by acquired drug resistance that limits overall therapeutic benefit.

Authors' Affiliation: Exelixis, Inc., South San Francisco, California

Received 9/18/07; revised 11/13/07; accepted 1/4/08.

The costs of publication of this article were defrayed in part by the payment of page charges. This article must therefore be hereby marked *advertisement* in accordance with 18 U.S.C. Section 1734 solely to indicate this fact.

Requests for reprints: Timothy S. Heuer, Molecular and Cellular Pharmacology, Exelixis, Inc., 210 East Grand Avenue, P. O. Box 511, South San Francisco, CA 94083. Phone: 650-837-8156; Fax: 650-837-7240; E-mail: theuer@exelixis.com.

doi:10.1158/1078-0432.CCR-07-4367

Resistance to kinase inhibitors can arise by mutation of the targeted kinase to cause interference of inhibitor activity or activation of alternate signaling pathways to relieve tumor growth addiction to the targeted kinase. The association of kinase mutations with therapeutic resistance to inhibitors of BCR-ABL (1–5), cKIT (6–10), platelet-derived growth factor receptor α (11), and epidermal growth factor receptor (EGFR; refs. 12–15) kinases is well established. Imatinib resistance via mutation of BCR-ABL in chronic myelogenous leukemia and mutation of cKIT in gastrointestinal stromal tumors provides a paradigm for the importance of kinase mutations as a mechanism for drug resistance and the clinical need for pharmacologic agents targeting a diverse range of mutant kinases. Next-generation ABL kinase inhibitors, including dasatinib and nilotinib, have been identified that inhibit imatinib-associated resistance mutations and offer promising therapies for chronic myelogenous leukemia patients (16–20). Similarly, defined resistance-associated mutation profiles are emerging in gastrointestinal stromal tumors following clinical treatment with imatinib and sunitinib (9, 21, 22). Several small-molecule EGFR-targeted drugs are emerging that inhibit the EGFR T790M mutation associated with resistance to erlotinib and gefitinib in non–small cell lung cancer, including

EXEL-7647 (23), BMS-690514 (24), and the irreversible inhibitor HKI-272 (25).

ErbB2 kinase domain mutations have been identified in human cancers originating from multiple tissues at a frequency of approximately 2% to 5% (26–31). Affected tumor types include breast, gastric, and ovarian carcinomas, non–small cell lung adenocarcinomas, and glioblastomas. The therapeutic relevance of the ErbB2 mutations remains to be determined, although many are homologous to known EGFR mutations that confer resistance to erlotinib and gefitinib. Documented mutations include single amino acid substitutions and short amino acid insertions. Mutations are found in structural regions of the kinase that could alter the kinase activation state, including the Cα-helix and activation loop. *In vitro*, the in-frame kinase domain YVMA insertion at G776 found in non–small cell lung adenocarcinomas is associated with increased ErbB2 kinase activity, potent cellular transformation, decreased potency of ErbB2 kinase inhibition by lapatinib, and resistance to the EGFR inhibitors gefitinib and erlotinib due to transphosphorylation of EGFR and ErbB3 (32). The established association of BCR-ABL, cKIT, platelet-derived growth factor receptor α, and EGFR kinase mutations with resistance to small-molecule kinase inhibitors provides examples of how cancer-associated ErbB2 mutations may affect the clinical benefit of ErbB2 inhibitors. Furthermore, the discovery of novel ErbB2 mutations associated with human tumors may accelerate with the advancement of ongoing cancer genome sequencing efforts as well as with the clinical administration of the recently approved small-molecule ErbB2 kinase inhibitor lapatinib (Tykerb; ref. 33). Knowledge of ErbB2 mutations that have the capacity to confer therapeutic resistance to lapatinib would provide valuable guidance as to potential mechanisms by which clinical resistance to lapatinib may arise, and allow for screening of novel small molecules that could inhibit lapatinib-resistant ErbB2 variants.

Here, we report the prospective discovery and characterization of ErbB2 mutations that confer resistance to lapatinib. ErbB2 mutations associated with lapatinib resistance were discovered by *in vitro* screening of a randomly mutagenized ErbB2 expression library in Ba/F3 cells that were dependent on ErbB2 activity for survival and growth. This approach has been used to discover clinically relevant BCR-ABL mutations that confer resistance to imatinib and dasatinib (34). In our studies, mutations at 16 different ErbB2 amino acid residues were associated with significant lapatinib resistance. The ErbB2 resistance-associated mutations were cloned and expressed to confirm that lapatinib resistance was conferred by the detected mutation. Mutation characterization using *in vitro* cell-based mechanistic and phenotypic studies showed that lapatinib resistance is correlated with sustained activation of ErbB2 and mitogen-activated protein kinase signaling in the presence of lapatinib and presents a potential direct mechanism for lapatinib drug resistance in ErbB2-driven tumors. EXEL-7647, a potent inhibitor of ErbB2, EGFR, and vascular endothelial growth factor receptor 2 receptor tyrosine kinases, retained significant activity against mutations associated with lapatinib resistance.

Materials and Methods

Reagents. Lapatinib was synthesized according to published methods (35). EXEL-7647 (23) was synthesized by the medicinal chemistry group at Exelixis, Inc.

Cell culture. GP2-293 cells were grown in DMEM with 10% fetal bovine serum (FBS), 100 units/mL penicillin, 100 units/mL streptomycin, and 0.1 mmol/L MEM nonessential amino acids (Mediatech, Inc.). Ba/F3 cells were grown in RPMI 1640 with 10% FBS, 1 ng/mL interleukin-3 (IL-3), and the supplements above. NIH-3T3 cells were grown in DMEM with 10% calf serum and the supplements above.

ErbB2 mutation library construction and resistance-associated mutation screening. ErbB2 random mutagenesis and resistance mutation screening were based on the protocol published by Azam et al. (34). ErbB2-V659E cDNA was cloned for cellular expression with a COOH-terminal FLAG tag by insertion into the *Bam*HI and *Eco*RI sites of the pRV2 vector to yield the pRV2-ErbB2-V659E construct. Plasmid DNA (1 μg) was used to transform the repair-deficient *Escherichia coli* strain XL-1 Red (Stratagene) according to the manufacturer's recommendations. Transformants were selected on Luria-Bertani agar plates with 100 μg/mL ampicillin (Fisher Scientific). Colonies were collected after 24 h and plasmid DNA was isolated using the EndoFree Plasmid Purification Mega kit (Qiagen) according to the manufacturer's procedures. The mutation rate was determined by DNA sequencing 70,000 bp and found to be 4.35×10^{-5}/bp.

For infection of Ba/F3 with ErbB2-expressing retrovirus, GP2-293 packaging cells (Clontech) were cotransfected with mutated pRV2-ErbB2-V659E cDNA and pVSV-G using FuGENE 6 transfection reagent (Roche) for the production of retrovirus. Retrovirus-containing supernatant was harvested 3 d after transfection with plasmid DNA, cleared by centrifugation in a tabletop centrifuge at 2,000 rpm for 5 min, and used to infect Ba/F3 cells. For retrovirus infection, the cleared supernatant was mixed 1:1 with RPMI 1640 that contained 2 ng/mL IL-3 and 16 μg/mL polybrene (Sigma). The infection mixture (12 mL) was added to 12×10^6 Ba/F3 cells that were harvested in log-phase growth by centrifugation at $1,500 \times g$ for 4 min. The cell suspension (1 mL) was transferred to each well of a 12-well tissue culture plate. The plate was subsequently centrifuged for 90 min with 2,500 rpm at 30°C in a Beckman Coulter Allegra 6R centrifuge. After centrifugation, the cells were incubated for 4 to 6 h at 37°C and then transferred to cell culture flasks containing fresh Ba/F3 cell medium.

Retrovirus-infected Ba/F3 cells were selected by growth in medium without IL-3. Twenty-four hours after retrovirus infection, IL-3 was removed by washing cells twice in RPMI 1640 with 10% FBS. After an additional 48 h, the cells were plated in soft agar medium containing 400 to 1,200 nmol/L lapatinib. To grow cells in soft agar medium, 2×10^6 to 8×10^6 cells were mixed with 9.6 mL RPMI 1640, 3.2 mL FCS, 3.2 mL of 1.5% agar in PBS, and varied concentrations of lapatinib (400, 800, or 1,200 nmol/L). The mixture was plated at 2 mL/well into six-well plates that had been precoated with 1 mL/well of the same mixture without cells. Twenty-four hours after cell plating, the wells were overlaid with 1 mL RPMI 1640 and 10% FBS containing the same drug concentration as the soft agar. After allowing 10 to 14 d for cell growth, single colonies of cells were picked and expanded separately in 2 mL RPMI 1640 and 10% FBS in the presence of 300 nmol/L lapatinib. Cells (48×10^6) were screened by this procedure. Screening for EXEL-7647 resistance was conducted in a similar manner. After expansion, genomic DNA was isolated using the DNeasy kit (Qiagen). The ErbB2 region from exons 11 to 27, corresponding to the juxtamembrane, kinase, and COOH-terminal domains, was amplified as the three overlapping PCR products using TaKaRa LA Taq DNA Polymerase (TaKaRa Bio USA) with the following PCR primers: ErbB2_ex11-19.F, 5′-TCCGGGGACGAATTCTGCACA-3′; ErbB2_ex11-19.R, 5′-TCACATTCTCCCCATCAGGGATCCA-3′; ErbB2_ex17-25.F, 5′-TCTTTGGGATCCTCATCAAG-3′; ErbB2_ex17-25.R, 5′-AGGGTCTGGACAGAAGAAGC-3′; ErbB2_ex24-27.F, 5′-ATTGACTCTGAATGTCGGCC-3′; ErbB2_ex24-27.R, 5′-CACTGGCACGTCCAGACCC-3′.

The resulting PCR products were sequenced bidirectionally using the following nested and internal sequencing primers: ErbB2_ex11-19.SF1, 5′-GGCGCCTACTCGCTGACCCTGC-3′; ErbB2_ex11-19.SR1, 5′-GCCAAAAGCGCCAGATCCAAGCA-3′; ErbB2_ex11-19.SF2,

5′-CTCAGTGACCTGTTTTGG-3′; ErbB2_ex11-19.SR2, 5′-AGGTCAGGTTTCACACCG-3′; ErbB2_ex17-25.SF1, 5′-CAGCAGAAGATCCGGAAGTA-3′; ErbB2_ex17-25.SR1, 5′-ATACTCCTCAGCATCCACCA-3′; ErbB2_ex17-25.SF2, 5′-GCCTCTTAGACCATGTCC-3′; ErbB2_ex17-25.SR2, 5′-ATCCTCCAGGTAGCTCATCC-3′; ErbB2_ex24-27.SF1, 5′-CGGGAGTTGGTGTCTGAATT-3′; ErbB2_ex24-27.SR1, 5′-CTCTGGGTTCTCTGCCGTAG-3′; ErbB2_ex24-27.SF2, 5′-AAGCCTCCCCACACATGACC-3′; ErbB2_ex24-27.SR2, 5′-TTCACATATTCAGGCTGG-3′.

Sequence analysis was done with the Phred/Phrap/Consed package (University of Washington, Seattle, WA).

Site-directed mutagenesis. Mutations identified in Ba/F3 cell viability screening were introduced into the appropriate constructs by site-directed mutagenesis using the QuikChange Site-Directed Mutagenesis kit (Stratagene) according to the manufacturer's instructions. Oligonucleotides for mutation insertion were designed using the Primer 3 program (Applied Biosystems, Inc.) and synthesized by Operon, Inc. Successful mutagenesis was confirmed in each case by DNA sequencing.

Cell viability assay. For drug treatment, Ba/F3 cells expressing mutant ErbB2 constructs were plated in 96-well plates at a concentration of 0.5×10^5 per well in 97 μL medium (RPMI 1640 containing 10% FBS but without IL-3). Serial 3-fold dilutions of lapatinib or EXEL-7647 in DMSO were prepared and further diluted 1:10 in RPMI 1640 for addition to the assay solution. RPMI 1640 – diluted compound (3 μL) was added per well, bringing the final reaction volume to 100 μL. Final drug concentrations in assay wells were 30,000, 10,000, 3,300, 1,100, 370, 123, 41, 14, 5, and 0 nmol/L. Assays were done in triplicate at each drug concentration. Forty-eight hours after compound addition, the number of viable cells was measured using the CellTiter-Glo assay (Promega) according to the manufacturer's instructions. Luminosity per well was determined using a Wallac multilabel counter (Perkin-Elmer), and the signal intensity was plotted versus drug concentration. The concentration of drug resulting in 50% inhibition of the maximum signal was determined, and this value is reported as the IC_{50}.

Focus formation assay. ErbB2 cDNA containing a COOH-terminal FLAG tag was cloned into the *Bam*HI and *Eco*RI sites of the pRV2 vector to yield the pRV2-ErbB2 construct. Individual mutations associated with drug resistance were introduced into the kinase domain of ErbB2 by site-directed mutagenesis as described above. Retrovirus production was done as described above. NIH-3T3 cells were infected with retrovirus as described above for Ba/F3 cells. To select retroviral-infected cells, puromycin was added 24 h after infection at a concentration of 1.2 ng/mL. Cells were harvested at ~70% confluency and plated in T75 flasks. Growth mode was documented by observation and photography, as cells were allowed to grow to ~95% confluency. Afterwards, the cells were lysed and genomic DNA was isolated. The presence of the mutation was confirmed by sequencing PCR products generated with primers directed against ErbB2 as described above.

Western blot analysis. Ba/F3 cells (3×10^6) in 9.7 mL of serum-free RPMI 1640 without IL-3 were plated per well in a 12-well tissue culture plate. Cells were incubated 2 h at 37°C, at which time 30 μL of lapatinib or EXEL-7647 (serum-free RPMI 1640 without IL-3) were added to each well for final concentrations of 30,000, 10,000, 3,300, 1,100, 370, 123, 41, 14, 5, and 0 nmol/L. Cells were collected by centrifugation 1 h after compound addition, washed with ice-cold PBS, and added to cell lysis buffer [50 mmol/L Tris-HCl (pH 7.4), 150 mmol/L NaCl, 1% NP40, 0.5% sodium deoxycholate, 0.1% SDS, 1 mmol/L sodium orthovanadate, 2 mmol/L phenylmethylsulfonyl fluoride, 10 mg/mL aprotinin, 5 mg/mL leupeptin, 1% phosphatase inhibitor cocktail I (Sigma)]. A protease inhibitor cocktail [1 Complete Mini with EDTA (Roche) per 10 mL] was added to the lysis buffer. Lysates were cleared by centrifugation and protein concentration was measured using the bicinchoninic acid protein assay (Pierce). NuPAGE SDS sample buffer (4×) and 10× NuPAGE sample reducing agent (Invitrogen) were added to lysates, which were then denatured for gel loading by incubation at 70°C for 10 min. Samples were loaded onto 4% to 12% NuPAGE Novex Bis-Tris gels and subjected to electrophoresis under denaturing conditions. Separated proteins were transferred to nitrocellulose according to the manufacturers' instructions (Invitrogen).

Protein blots were probed with antibodies against phosphorylated ErbB2 (pErbB2; Cell Signaling), FLAG (Sigma) for measurement of total ErbB2, phosphorylated extracellular signal-regulated kinase (pERK; Cell Signaling), and ERK (Cell Signaling). Horseradish peroxidase – labeled secondary antibodies (Jackson ImmunoResearch Laboratories) were used for detection of primary antibodies, with the exception of the FLAG antibody, which was directly coupled to horseradish peroxidase. Horseradish peroxidase was visualized using enhanced chemiluminescence plus chemiluminescent substrate and a Typhoon imager (both from GE Healthcare).

Computer structural modeling. ErbB2 wild-type (WT) and mutant protein structures were generated using the homology modeling tools associated with MOE (version 2006.08; Chemical Computing Group). Template structures included both public [Protein Data Bank codes: 1M17 (36), 1XKK (37), 2GS6 (38), and 2GS7 (38)] and proprietary EGFR crystal structures. Ligand docking experiments used Glide (version 4.5) available from Schrodinger. Molecular graphics were created using PyMOL (version 0.98; DeLano Scientific LLC).

Results

Identification of ErbB2 mutations associated with lapatinib resistance. Ba/F3 cells can be engineered to grow in the absence of IL-3 by transgenic expression of kinases that promote cytokine-independent activation of growth and survival signal transduction pathways. For example, BCR-ABL expression induces STAT phosphorylation and signaling to confer cytokine-independent growth of Ba/F3 cells (34). In our studies, Ba/F3 cells were made to express the V659E mutant of ErbB2 by retroviral infection of a cytomegalovirus promoter – driven ErbB2 V659E expression clone, and infected cells showed robust growth in the absence of exogenous cytokine. The V659E mutant of ErbB2 was selected because it is a well-characterized mutation in the transmembrane domain of ErbB2 known to confer constitutive kinase activity and transform NIH-3T3 cells (39, 40). The ErbB2 V659E expression clone was subjected to random mutagenesis by passaging the vector in DNA repair – deficient *E. coli*. DNA sequence analysis determined the mutation frequency of the mutagenized ErbB2 expression library to be 4.35×10^{-5}/bp. This ErbB2 V659E random mutation library was expressed in Ba/F3 cells by retroviral infection and screened for mutations that sustained lapatinib-resistant growth (Fig. 1).

Ba/F3 cells expressing randomly mutated ErbB2 survived and grew in the presence of various lapatinib concentrations (400, 600, 800, and 1,200 nmol/L) that prevented growth of unmutagenized ErbB2-expressing cells. Multiple independent rounds of screening for resistance-associated mutations were completed in soft agar medium without IL-3. Amino acid substitution mutations were identified by DNA sequencing in 122 of 125 colonies selected by lapatinib-resistant growth. In the lapatinib-resistant Ba/F3 clones, 17 different single amino acid substitutions were identified at 16 amino acid locations (Table 1; Fig. 2). Mutations were isolated repeatedly in multiple independent clones, which indicated that screening saturation was achieved. Two of the 17 amino acid substitutions have been identified in clinical tumors at a low frequency; however, these mutations were not previously associated with drug resistance. L755S was reported in gastric and breast tumors, and T733I was reported in gastric tumors (29). Mutations

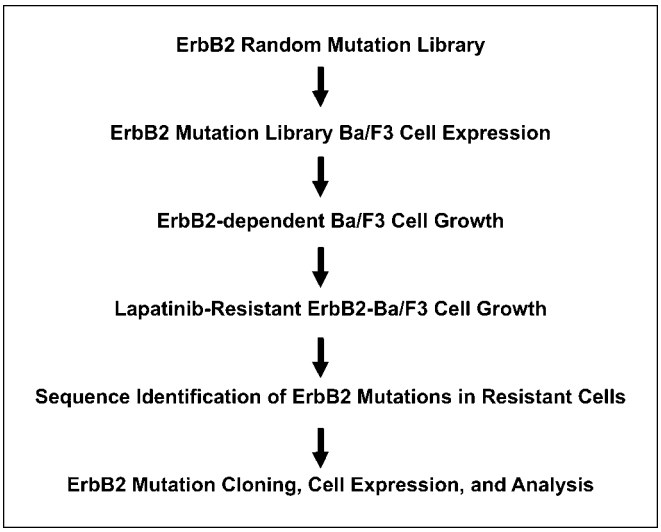

Fig. 1. Schematic of the *in vitro* screen for ErbB2 drug resistance – associated mutations. An ErbB2 V659E expression construct was subjected to random mutagenesis. Cells expressing mutated ErbB2 that survived and grew in the presence of lapatinib or EXEL-7647 concentrations that prevented growth of cells expressing unmutagenized ErbB2 were selected and resistance-associated mutations were identified by DNA sequencing. The ErbB2 resistance-associated mutations were cloned and expressed in Ba/F3 cells to confirm that drug resistance was conferred by the detected mutation. Following stable expression of the mutated ErbB2 protein, survival IC_{50} values for all mutations and phosphorylation IC_{50} values for selected mutations were determined from 10-point dose-response assays.

were most prevalent in the ErbB2 kinase domain (12 of the 17 mutations). The remaining five mutations were found in the juxtamembrane domain (three), extracellular domain (one), and COOH-terminal domain (one) of ErbB2.

Lapatinib-resistant colonies were also isolated that contained double and triple ErbB2 mutation combinations. In addition to the 17 mutations we report identified as single mutations, 10 unique amino acid substitutions were discovered in different double and triple mutation combinations. The mutations were believed to be passengers rather than resistance driver mutations because each of the 10 mutations was identified in combinations that included a mutation discovered independently in singlet form. However, we cannot exclude the possibility that these additional mutations may also enhance the overall fitness of ErbB2 kinase activity.

Resistance mutation cloning and cell expression recapitulates drug resistance. The ErbB2 resistance-associated mutations identified in screens of the ErbB2 random mutation library were cloned and expressed in Ba/F3 cells to confirm that lapatinib resistance was conferred by the detected mutation. Following stable expression of the mutated ErbB2 protein, lapatinib survival IC_{50} values for all mutations were determined from a 10-point dose-response cell viability assay (Table 1). Lapatinib survival IC_{50} values were >1,000 nmol/L for 6 of 17 mutations and >400 nmol/L for 11 of 17 mutations. The highest survival IC_{50} values, which correspond to the highest levels of drug resistance, were found for mutations isolated most frequently in our screens. ErbB2 T798I, isolated in 35 independent clones, showed the highest lapatinib survival IC_{50} with a value of 3,339 nmol/L. Lapatinib-induced non–ErbB2-mediated toxicity is ~3,000 nmol/L in parental Ba/F3 cells; hence, the 3,339 nmol/L IC_{50} for survival of ErbB2 T798I–expressing Ba/F3 cells in the presence of lapatinib suggests that lapatinib-induced cell death was independent of ErbB2 inhibition for these cells. Mutations that conferred lapatinib viability IC_{50} values near the level of ErbB2-independent cytotoxicity

Table 1. ErbB2 mutations associated with lapatinib resistance and survival IC_{50} analysis of cloned ErbB2 resistance-associated mutations expressed in Ba/F3 cells

ErbB2 mutation	Clones	Mutation frequency (%)	Protein domain	Ba/F3 cell line	Lapatinib		EXEL-7647	
					IC_{50} (nmol/L)	SD	IC_{50} (nmol/L)	SD
None	NA	NA	NA	V659E	96	21	148	25
C630Y	1	1.1	EC	—	—	—	—	—
E717K	1	1.1	JM	V659E_E717K	461	50	294	103
E719K	1	1.1	JM	—	—	—	—	—
E719G	1	1.1	JM	V659E_E719G	894	162	43	6
L726F	8	9.0	Kinase	V659E_L726F	1,056	65	315	88
T733I	2	2.2	Kinase	V659E_T733I	670	25	515	153
L755S	5	5.6	Kinase	V659E_L755S	2,861	746	371	13
P780L	4	4.5	Kinase	V659E_P780L	1,127	76	448	129
S783P	5	5.6	Kinase	V659E_S783P	3,273	5	181	61
L785F	15	16.9	Kinase	V659E_L785F	1,154	65	554	175
T798I	35	39.3	Kinase	V659E_T798I	3,339	289	419	131
Y803N	1	1.1	Kinase	V659E_Y803N	496	170	123	24
E812K	6	6.7	Kinase	V659E_E812K	407	74	187	1
D821N	1	1.1	Kinase	V659E_D821N	249	5	318	49
V839G	1	1.1	Kinase	V659E_V839G	286	14	96	8
L915M	1	1.1	Kinase	V659E_L915M	253	53	152	89
S1002R	1	1.1	CT	—	—	—	—	—

NOTE: Mutations identified by DNA sequencing in lapatinib-resistant cells were introduced into ErbB2 V659E expression constructs by site-directed mutagenesis to resynthesize the resistance-associated mutations. The mutant ErbB2 constructs were expressed in Ba/F3 cells, and stable expressing cells were selected. Cell viability was measured following 48-h compound treatment in the absence of IL-3. Viability IC_{50} values were calculated from a 10-point lapatinib or EXEL-7647 dose response.
Abbreviations: EC, extracellular; JM, juxtamembrane; CT, COOH terminus.

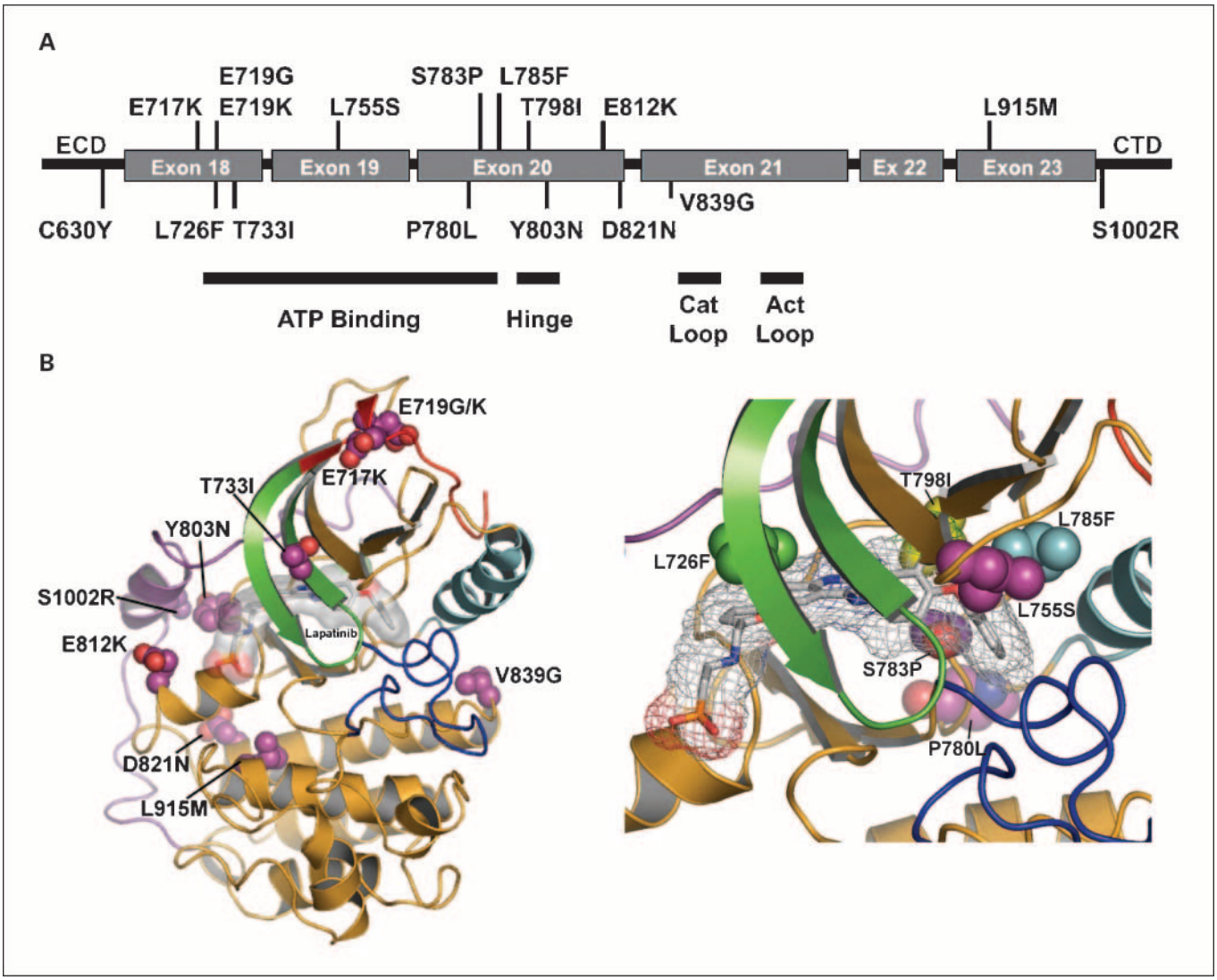

Fig. 2. *A,* a schematic of the ErbB2 juxtamembrane and kinase domains shows the resistance-associated mutations identified in our studies. Functional domains are indicated. Seventeen different single amino acid substitutions, which map to 16 ErbB2 amino acid residues, are marked at the corresponding sequence positions. L785F was identified in both lapatinib and EXEL-7647 screens. *B,* amino acids where resistance-associated substitution mutations were identified are shown on an ErbB2 structural model. The model shown is an inactive form of the ErbB2 kinase domain with lapatinib docked in the ATP-binding site. The box shows a magnification of the ATP-binding region. Blue, activation loop; cyan, Cα-helix; green, nucleotide-binding loop; red, NH_2-terminal extension; pink, COOH-terminal extension.

were T798I, L755S, and S783P. Additional ErbB2 mutations associated with lapatinib viability IC_{50} values >1,000 nmol/L were L726F, P780L, and L785F (Table 1). Recently, it was reported that ErbB2 L726I causes resistance to gefitinib (41).

In contrast, the EGFR/ErbB2/vascular endothelial growth factor receptor inhibitor EXEL-7647 was found to inhibit mutant forms of ErbB2 associated with lapatinib resistance. EXEL-7647 cell viability IC_{50} values were <555 nmol/L for all 17 ErbB2 mutations and were <400 nmol/L for 13 of 17 mutations. The highest EXEL-7647 viability IC_{50} was associated with the L785F mutation (554 nmol/L; Table 1). EXEL-7647 viability IC_{50} values for the identified ErbB2 mutations were consistent with results from resistance screens. In multiple independent screens using EXEL-7647, viable cells were difficult to isolate. Several cell colonies were formed in the presence of 600 nmol/L EXEL-7647 and found to express the L785F substitution, which was also identified repeatedly in lapatinib resistance mutation screens. Notably, repeated screen attempts were unable to discover any ErbB2 mutations associated with EXEL-7647 resistance and lapatinib sensitivity.

Sustained ErbB2 phosphorylation in cells expressing ErbB2 resistance-associated mutations correlates with cell viability. To investigate the mechanism of drug resistance associated with the ErbB2 mutations, levels of ErbB2 expression were examined and phosphorylation IC_{50} values for selected mutations were determined from a 10-point dose-response Western blot analysis (Table 2; Fig. 3). The expression level of ErbB2 was not correlated with drug resistance. In general, alignment between survival and phosphorylation IC_{50} values was observed, and ErbB2 and ERK phosphorylation IC_{50} values agreed; however, most phosphorylation IC_{50} values were elevated compared with survival IC_{50} values. Lapatinib ErbB2 phosphorylation IC_{50} values were 3,610 and 3,918 nmol/L for L755S and L785F resistance-associated mutations, which have survival IC_{50} values of 2,861

Table 2. IC_{50} values for cell viability, ErbB2 phosphorylation, and ERK phosphorylation

Ba/F3 cell line	Resistance mutation	Survival IC_{50} (nmol/L)		pErbB2 IC_{50} (nmol/L)		pERK IC_{50} (nmol/L)	
		Lapatinib	EXEL-7647	Lapatinib	EXEL-7647	Lapatinib	EXEL-7647
V659E	None	96	148	742	983	1,259	559
V659E_L755S	L755S	2,861	371	3,610	954	9,375	1,248
V659E_L785F	L785F	1,154	554	3,918	3,341	10,107	5,966
V659E_T798I	T798I	3,339	419	>30,000	3,267	>30,000	3,296

and 1,154 nmol/L, respectively. The lapatinib ErbB2 phosphorylation IC_{50} for the T798I mutation was >30,000 nmol/L, which was consistent with a survival IC_{50} value independent of ErbB2 inhibition. EXEL-7647 ErbB2 phosphorylation IC_{50} values for T798I and L785F mutations were 3,267 and 3,341 nmol/L, respectively. The basis for elevated ErbB2 phosphorylation IC_{50} values compared with the cytokine-independent cell survival IC_{50} values is not clear but could include differences in assay sensitivity and kinetics. The phosphorylation data indicate that <50% inhibition of ErbB2 activity is required for inhibition of cell survival in the absence of IL-3 and that survival is correlated with ErbB2 kinase activity.

The most frequently identified ErbB2 mutation to confer lapatinib resistance, T798I, is a residue of highly conserved function in protein kinases. The amino acid in this position has become known as the gatekeeper residue because of its location near the ATP-binding site and association with drug resistance in multiple protein kinases, including EGFR, BCR-ABL, and cKIT (42). Mutations at the analogous residue in BCR-ABL and cKIT have been discovered in clinical tumors that are highly resistant to imatinib (2, 6). Similarly, mutation of the EGFR gatekeeper residue has been discovered in association with resistance to erlotinib and gefitinib in non–small cell lung tumors (13, 14). The ErbB2 T798I–expressing Ba/F3 cells survive and grow in the presence of lapatinib up to concentrations that cause toxicity that is unrelated to ErbB2 inhibition, and have corresponding IC_{50} values for survival (3,339 nmol/L) and ErbB2 phosphorylation (>30,000 nmol/L;

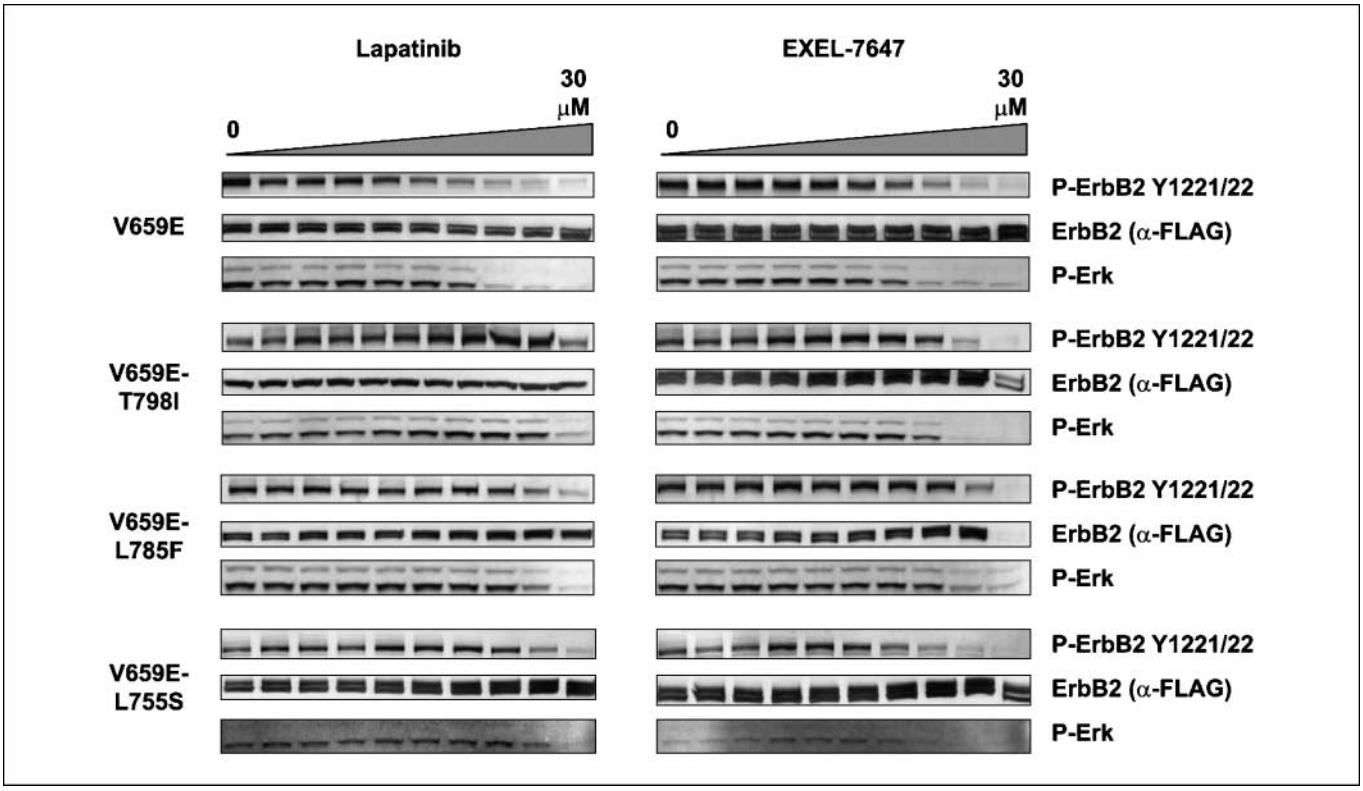

Fig. 3. Expression of mutant ErbB2 in Ba/F3 cells and determination of phosphorylation IC_{50} values. Ba/F3 cells selected for stable expression of resistance-associated mutations were used for ErbB2 and ERK phosphorylation IC_{50} determination. Cells were transferred to medium without serum or IL-3 2 h before compound addition. Following 1-h compound treatment (30,000, 10,000, 3,300, 1,100, 370, 123, 41, 14, 5, and 0 nmol/L), cells were harvested for Western blot analysis of pErbB2, total ErbB2 (FLAG), pERK, and total ERK. IC_{50} values were determined from a 10-point lapatinib or EXEL-7647 dose response. Western blot images of pErbB2, ErbB2, and pERK from cells expressing ErbB2 V659E, ErbB2 V659E.T798I, ErbB2 V659E.L785F, or ErbB2 V659E.L755S. IC_{50} values for pErbB2 were calculated using pErbB2 intensity after normalization to total ErbB2 levels. IC_{50} values for pERK were calculated using pERK intensity after normalization to total actin levels (data not shown). At least two immunoblot experiments were completed, and representative data are shown. The decreased ErbB2 protein level observed with 30 μmol/L EXEL-7647 treatments was associated with cell death (this effect was diminished in some samples by normalized protein loading).

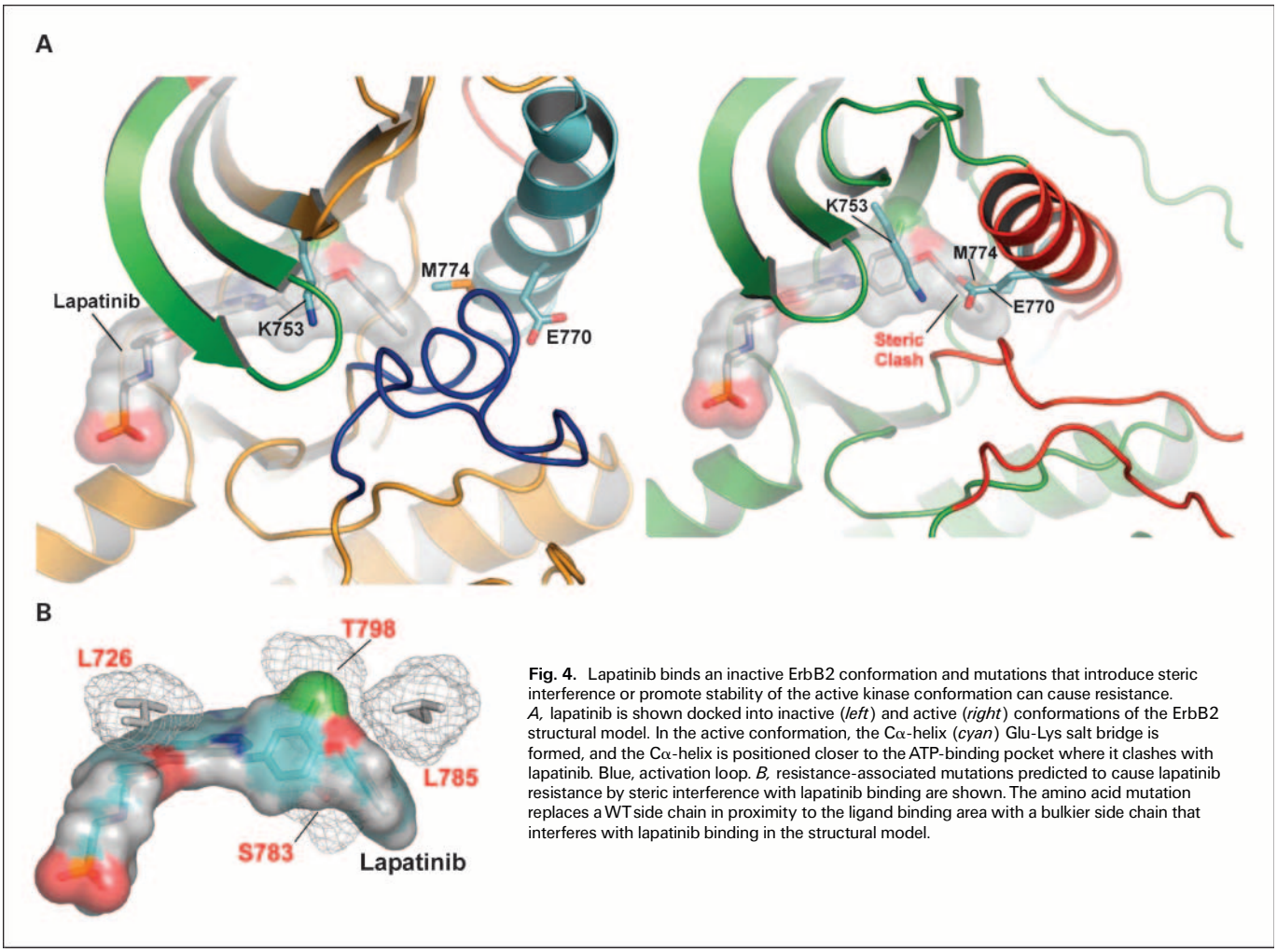

Fig. 4. Lapatinib binds an inactive ErbB2 conformation and mutations that introduce steric interference or promote stability of the active kinase conformation can cause resistance. *A,* lapatinib is shown docked into inactive (*left*) and active (*right*) conformations of the ErbB2 structural model. In the active conformation, the Cα-helix (*cyan*) Glu-Lys salt bridge is formed, and the Cα-helix is positioned closer to the ATP-binding pocket where it clashes with lapatinib. Blue, activation loop. *B,* resistance-associated mutations predicted to cause lapatinib resistance by steric interference with lapatinib binding are shown. The amino acid mutation replaces a WT side chain in proximity to the ligand binding area with a bulkier side chain that interferes with lapatinib binding in the structural model.

Table 2; Fig. 3). The lapatinib resistance associated with ErbB2 T798I parallels the EGFR T790M resistance profile for gefitinib, erlotinib, and lapatinib. Lapatinib resistance to EGFR T790M and EGFR L777F, which is homologous to ErbB2 L785F, was shown by cloning and expression of the mutated EGFR variants in 293 cells for EGFR autophosphorylation analysis. Lapatinib was unable to inhibit EGFR T790M or L777F; autophosphorylation IC_{50} values were >30,000 nmol/L for both mutations (data not shown).

An inactive conformation of the ErbB2 Cα-helix is required for lapatinib binding. By analogy with the structure of EGFR, lapatinib is expected to bind competitively with ATP in the ErbB2 nucleotide-binding pocket (37). To correlate resistance mutations with lapatinib binding, structural models of the ErbB2 kinase domain were constructed using crystal structures of the homologous EGFR (36). Lapatinib binding is compatible only with an inactive conformation of the ErbB2 kinase in which the Cα-helix is positioned away from the nucleotide-binding pocket with the Glu-Lys salt bridge not formed (Fig. 4A). The structural model suggests that amino acid changes near the ATP-binding pocket that introduce direct steric interference with lapatinib binding, or changes that promote movement of the Cα-helix into the nucleotide-binding pocket (which is required for kinase activation) can block binding of lapatinib to ErbB2.

ErbB2 mutations associated with the highest lapatinib resistance clustered in the NH_2-terminal kinase lobe and hinge region and included L726F, L755S, P780L, S783P, L785F, and T798I. The L726F, L785F, S783P, and T798I mutations are expected to act by direct steric interference (Fig. 4B). The L726F and L785F mutations replace the aliphatic side chain of leucine with the rigid, bulkier phenylalanine side chain. The threonine to isoleucine substitution at T798 results in increased bulk and loss of a polar oxygen atom. ErbB2 residues L726F and S783P associated with lapatinib resistance have spatially homologous residues in the ABL kinase associated with imatinib resistance: L248R, Q252H (ErbB2 L726), and V299L (ErbB2 S783).

Mutations at L755S or P780L are expected to directly shift the activation state dynamics to favor a conformation where the Cα-helix is positioned to block lapatinib binding, and represent the class of mutations believed to cause resistance by constraining kinase conformational flexibility. The leucine at L755 is predicted to participate in hydrophobic interactions with leucine residues of the activation loop. Substitution of the nonpolar leucine side chain with the smaller, polar serine group is expected to disrupt hydrophobic activation loop packing interactions that result in destabilization of an inactive conformation required for lapatinib binding. Structural modeling was unable to suggest a specific mechanism for the resistance associated with several mutations, such as C630Y,

E717K, E719K/E719G, Y803N, E812K, D821N, and S1002R. These mutations may restrict conformational flexibility or otherwise affect the structure such that the inactive conformations required for lapatinib binding are unfavorable.

ErbB2 mutations are associated with lapatinib resistance and cellular transformation. To assess the transforming capability of kinase domain mutations associated with lapatinib resistance, the mutations were cloned and expressed in the absence of the V659E activating mutation and investigated for the ability to induce foci *in vitro*. Mutants that activate ErbB2 and promote oncogenic transformation have an intrinsic mechanism for growth selection before the tumor is exposed to selective pressure with an ErbB2 inhibitor. Resistance-associated mutations identified in our studies that also are associated with kinase activation and oncogenic transformation may have particular clinical relevance.

Resistance-associated mutations that mapped to the kinase domain were expressed individually in the context of an otherwise WT ErbB2 amino acid sequence and analyzed for focus formation in NIH-3T3 cells. Assays were conducted with cells stably expressing WT or mutated ErbB2 protein, which were constructed by infection of 3T3 cells with retrovirus expressing ErbB2. Cells expressing mutated ErbB2 variants were sequenced to confirm the mutation status. NIH-3T3 cells grew in a monolayer in the absence of ErbB2 transgene expression (Fig. 5A) but formed foci of aggregated, transformed cells when expressing ErbB2 V659E (Fig. 5B), in accordance with published data (39, 40). WT ErbB2 had no effect on the formation of foci with NIH-3T3 cells (Fig. 5C). The T798I mutant, which was the most frequently observed mutation in screens done with lapatinib, also failed to transform NIH-3T3 cells in this assay. We also constructed the analogous EGFR T790M variant and found that it too was not transforming (data not shown).

In contrast, NIH-3T3 cells expressing the L755S mutant form of ErbB2, which was associated with high-level lapatinib resistance, formed growth foci comparable with ErbB2 V659E (Fig. 5D). The transformation effect of ErbB2 L755S on NIH-3T3 cell growth was consistent with structural modeling results showing L755 participates in hydrophobic packing interactions that stabilize the kinase activation loop in an inactive conformation. Additional mutations associated with lapatinib resistance that were active in NIH-3T3 cell foci formation were T733I and D821N, although the appearance of foci with T733I or D821N occurred less frequently than with L755S or V659E. The T733I and D821N mutations were considered weakly transforming in our assay. The observation that L755S and T733I are transforming mutations associated with clinical tumors and *in vitro* lapatinib resistance provides evidence that our screen discovered ErbB2 mutations that may have clinical relevance for drug resistance.

Discussion

Our studies investigated ErbB2 mutations that cause resistance to kinase inhibition by lapatinib. A Ba/F3 cell-based system that required ErbB2 kinase activity for cell viability was engineered and used to screen a library of random ErbB2 mutations. This approach has been used with success by others to screen for mutations associated with BCR-ABL resistance to imatinib and dasatinib (34) as well as FLT3 resistance to PKC-412 (43). Our ErbB2 mutation screens revealed 17 different ErbB2 amino acid substitutions, involving 16 different residues associated with lapatinib resistance. EXEL-7647 was found to have significant activity against most of the mutations associated with lapatinib resistance, and ErbB2 mutations associated with EXEL-7647 resistance and lapatinib sensitivity were not discovered in multiple independent screen attempts.

The chemical structure and mode of drug binding to a kinase influence the vulnerability of a kinase inhibitor to target-directed mutational resistance (5). Drugs such as lapatinib and

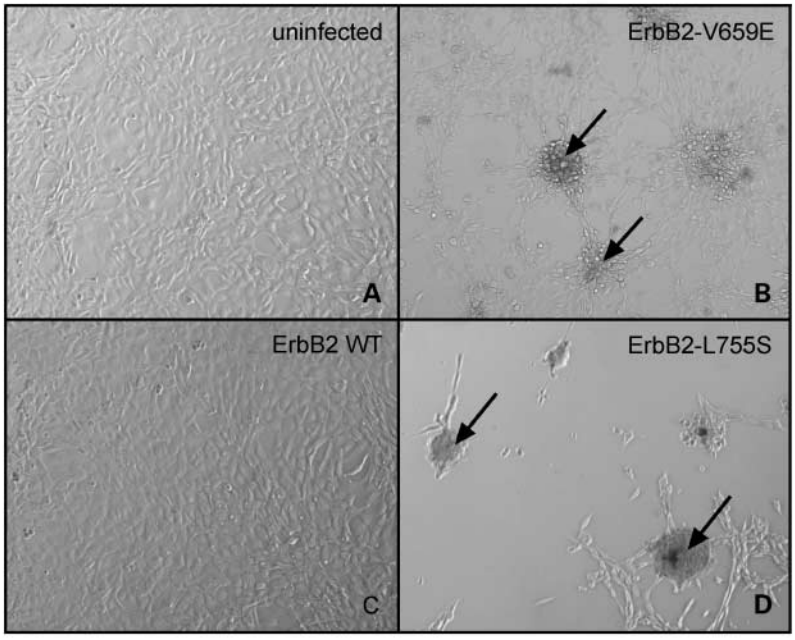

Fig. 5. ErbB2 drug resistance – associated mutations are transforming in NIH-3T3 cells. Mutations identified by DNA sequencing in lapatinib-resistant cells were introduced into WT ErbB2 expression constructs by site-directed mutagenesis to resynthesize the resistance-associated mutations in the absence of the V659E primary mutation. The mutant ErbB2 constructs were expressed in NIH-3T3 cells and stable expressing cells were selected. Cells were grown to confluence. Growth mode was documented by observation and photography. *A,* uninfected NIH-3T3 cells grow to confluence and form a monolayer. *B,* NIH-3T3 cells expressing ErbB2 V659E fail to reach confluence and form foci of piled-up cells. *C,* NIH-3T3 cells expressing WT ErbB2 grow to confluence and form a monolayer as observed for uninfected cells. *D,* NIH-3T3 cells expressing ErbB2 L755S fail to reach confluence and form foci of piled-up cells as observed for ErbB2 V659E.

imatinib that are restricted to binding an inactive structural conformation of the kinase have increased susceptibility to resistance mutations because mutations that shift the conformational dynamics to favor an active conformation confer resistance. In our studies, the ErbB2 L755S mutation illustrates resistance via restriction of kinase conformational flexibility. Structural modeling of WT ErbB2 predicts that L755 makes tight hydrophobic interactions with activation loop leucine side chains that stabilize an inactive kinase conformation. Serine at residue 755 would disrupt hydrophobic packing and alter the thermodynamic equilibrium to favor a conformation in which the activation loop and Cα-helix adopt positions required for kinase activity and that are incompatible with lapatinib binding. L755S was associated with high levels of lapatinib resistance, marked by IC_{50} values >3,000 nmol/L in both cell viability and ErbB2 autophosphorylation assays.

Mutations that act via direct steric interference to prevent drug binding can cause resistance to drugs that bind to both active and inactive kinase structural conformations. In the case of ATP-competitive kinase inhibitors, mutations that block drug binding by steric interference must not impair ATP-binding or kinase activity. The gatekeeper residue of protein kinases, located at the boundary of the ATP-binding region, is the canonical site of amino acid substitution representing this class of resistance-associated mutation (42). In our studies, the T798I ErbB2 gatekeeper mutation was the most frequently identified mutation in lapatinib resistance screens and was associated with the highest level of lapatinib resistance. Lapatinib failed to inhibit ErbB2 T798I autophosphorylation at a 30,000 nmol/L concentration, and lapatinib-induced death of Ba/F3 cells expressing ErbB2 T798I was independent of ErbB2 inhibition. A T790M mutation at the analogous residue in EGFR is associated with clinical resistance to gefitinib and erlotinib. ErbB2 T798I and EGFR T790M mutations have comparable levels of resistance to lapatinib and provide evidence that ErbB2 T798I may have clinical relevance for lapatinib resistance. EXEL-7647 was shown previously to inhibit the EGFR T790M variant (23): in the present study, we also show that ErbB2 T798I is susceptible to inhibition by EXEL-7647.

The resistance-associated mutation profiles for lapatinib-ErbB2 and imatinib-BCR-ABL share important features, including the association of numerous mutations with resistance to each drug and two general mechanisms of action for resistance-associated mutations: direct steric interference with drug binding and shifting conformational equilibrium toward the active state. Both lapatinib and imatinib bind exclusively to the inactive conformations of ErbB2 and ABL kinases, respectively, and this conformational dependence most likely confers resistance susceptibility to multiple mutations that promote the active conformation. In contrast to lapatinib and imatinib, EXEL-7647 inhibits both active and inactive kinase conformations and inhibits mutant forms of ErbB2 associated with lapatinib resistance. Although multiple determinants influence whether kinase mutations confer resistance to small-molecule inhibitors, including drug potency and binding kinetics, our findings support the conclusion that kinase inhibitors limited to binding inactive kinase conformations are likely to have increased susceptibility to target-associated resistance mutations (15).

The clinical relevance of the mutations discovered in our *in vitro* screen will be tested as ErbB2 inhibitors such as lapatinib gain use as clinical therapeutics. Lapatinib was recently approved as a second-line therapy in combination with capecitabine in HER2-positive, metastatic breast cancer (33, 44), although no data are yet available on clinical resistance to lapatinib involving ErbB2 mutations. Two lapatinib-resistant mutants discovered in our screen, L755S and T733I, have been identified previously in breast and gastric tumors and thus are examples of established cancer-associated mutations. Three mutations from our resistance screen, including L755S and T733I, were shown to be transforming in an *in vitro* foci formation growth assay, presenting evidence that the resistance-associated mutations can play a driving role in tumor growth phenotypes and have the capacity to arise as primary tumor-associated resistance mutations. However, the T798I variant (the most frequent mutation recovered in screens with lapatinib) did not have transforming properties nor did the analogous T790M mutation in EGFR. The T790M EGFR mutation has been described as having enhanced kinase activity and providing a proliferative advantage in cells overexpressing this variant (45). Our data suggest that this enhanced activity is not sufficient to be transforming by itself, although the profound resistance to lapatinib conferred by this substitution leads to strong selective pressure in the resistance screens. Consistent with this, it was recently reported that EGFR T790M does not transform NIH-3T3 cells, although it shows relatively modest enhancement of kinase activity that dramatically potentiates other activating mutations in EGFR (46).

It is unknown how the level of kinase activation required for activity in the *in vitro* foci formation assay relates to the degree of activation needed for tumor-associated growth selection in the absence of a kinase inhibitor. The level of kinase activation that confers a tumor growth advantage, and enables subpopulations of tumor cells with resistance-associated mutations to exist before inhibitor-induced selection, likely will vary with the genetic complexity of tumors. Our *in vitro* foci formation assay did not attempt to model the genetic complexity and diversity of human tumors, and formation of foci in our assay may be expected to require a higher level of kinase activation than that needed to affect growth of human tumors with complex genetic alterations. Consequently, it remains plausible that resistance-associated mutations failing to induce NIH-3T3 cell foci formation *in vitro* may activate kinase activity and affect human tumor growth phenotypes.

The diversity of mutations identified in our screens and the absence of nonmutation-associated resistance indicates that ErbB2 mutation may be a prominent mechanism for ErbB2-driven tumors to evade inhibition by lapatinib. Nonmutation mechanisms for drug resistance have been described for kinase inhibition, including ErbB2 and EGFR inhibitors, and do provide alternate survival pathways for tumors to evade therapeutic efficacy. Activation of estrogen receptor has been implicated in resistance to lapatinib, and lapatinib has been shown to induce estrogen receptor expression in patients receiving lapatinib therapy (47). Activation of phosphatidylinositol 3-kinase/AKT signaling via PTEN loss (48–51) or increased ErbB3 transphosphorylation (52) has also been shown to confer resistance to ErbB2 inhibition. Similarly, activation of cMET by gene amplification activates ErbB3 signaling and provides an escape mechanism to EGFR inhibition by gefitinib that is sensitive to inhibitors of MET kinase activity (53). Restoration of PTEN activity or inhibition

of phosphatidylinositol 3-kinase/AKT (54), as well as inhibition of mammalian target of rapamycin (55), restores sensitivity in PTEN/phosphatidylinositol 3-kinase/AKT–mediated resistance. The manifestation of clinical therapeutic resistance in tumors under ErbB2 drug therapy is likely to involve multiple pathways and will be dependent on the composite genetic makeup of the tumor and associated therapeutic selective pressure. Our studies show that kinase mutations can provide a facile resistance mechanism for the small-molecule ErbB2 inhibitor lapatinib, and describe a resistance-associated mutation profile for lapatinib involving mutations that result in high-level resistance and promote cellular neoplastic transformation *in vitro*.

EXEL-7647, a potent inhibitor of ErbB2, EGFR, and vascular endothelial growth factor receptor 2 receptor tyrosine kinases, retains activity against the broad spectrum of ErbB2 mutations that confer resistance to lapatinib inhibition. The L785F mutation was associated with the most significant resistance to EXEL-7647, and as observed for the other mutant forms of ErbB2 identified in our resistance screens, this mutant was more sensitive to EXEL-7647 than to lapatinib. EXEL-7647 binds both active and inactive conformations of ErbB2, which may allow EXEL-7647 to retain activity against mutations that promote kinase activation and contribute to the contrasting resistance mutation profiles for lapatinib and EXEL-7647. Based on the results reported here and in previous studies (23), we speculate that EXEL-7647 may be able to circumvent some of the target-associated resistance mechanisms associated with lapatinib.

Acknowledgments

We thank the many people within Exelixis Drug Discovery and Translational Medicine whose support and contributions enabled these studies, with particular recognition to Edith Ubannwa.

References

1. Shah NP. Loss of response to imatinib: mechanisms and management. Hematology Am Soc Hematol Educ Program 2005;1:183–7.
2. Shah NP, Nicoll JM, Nagar B, et al. Multiple BCR-ABL kinase domain mutations confer polyclonal resistance to the tyrosine kinase inhibitor imatinib (STI571) in chronic phase and blast crisis chronic myeloid leukemia. Cancer Cell 2002;2:117–25.
3. Wadleigh M, DeAngelo DJ, Griffin JD, Stone RM. After chronic myelogenous leukemia: tyrosine kinase inhibitors in other hematologic malignancies. Blood 2005;105:22–30.
4. Soverini S, Martinelli G, Colarossi S, et al. Second-line treatment with dasatinib in patients resistant to imatinib can select novel inhibitor-specific BCR-ABL mutants in Ph+ ALL. Lancet Oncol 2007;8:273–4.
5. Burgess MR, Skaggs BJ, Shah NP, Lee FY, Sawyers CL. Comparative analysis of two clinically active BCR-ABL kinase inhibitors reveals the role of conformation-specific binding in resistance. Proc Natl Acad Sci U S A 2005;102:3395–400.
6. Antonescu CR, Besmer P, GuoT, et al. Acquired resistance to imatinib in gastrointestinal stromal tumor occurs through secondary gene mutation. Clin Cancer Res 2005;11:4182–90.
7. Chen LL, Sabripour M, Andtbacka RH, et al. Imatinib resistance in gastrointestinal stromal tumors. Curr Oncol Rep 2005;7:293–9.
8. Debiec-Rychter M, Dumez H, Judson I, et al. Use of c-KIT/PDGFRA mutational analysis to predict the clinical response to imatinib in patients with advanced gastrointestinal stromal tumours entered on phase I and II studies of the EORTC Soft Tissue and Bone Sarcoma Group. Eur J Cancer 2004;40:689–95.
9. Heinrich MC, Corless CL, Blanke CD, et al. Molecular correlates of imatinib resistance in gastrointestinal stromal tumors. J Clin Oncol 2006;24:4764–74.
10. Heinrich MC, Corless CL, Demetri GD, et al. Kinase mutations and imatinib response in patients with metastatic gastrointestinal stromal tumor. J Clin Oncol 2003;21:4342–9.
11. Corless CL, Schroeder A, Griffith D, et al. PDGFRA mutations in gastrointestinal stromal tumors: frequency, spectrum and *in vitro* sensitivity to imatinib. J Clin Oncol 2005;23:5357–64.
12. Jackman DM, Yeap BY, Sequist LV, et al. Exon 19 deletion mutations of epidermal growth factor receptor are associated with prolonged survival in non-small cell lung cancer patients treated with gefitinib or erlotinib. Clin Cancer Res 2006;12:3908–14.
13. Kobayashi S, Boggon TJ, Dayaram T, et al. EGFR mutation and resistance of non-small-cell lung cancer to gefitinib. N Engl J Med 2005;352:786–92.
14. Pao W, Miller VA, Politi KA, et al. Acquired resistance of lung adenocarcinomas to gefitinib or erlotinib is associated with a second mutation in the EGFR kinase domain. PLoS Med 2005;2:e73.
15. Balak MN, Gong Y, Riely GJ, et al. Novel D761Y and common secondary T790M mutations in epidermal growth factor receptor-mutant lung adenocarcinomas with acquired resistance to kinase inhibitors. Clin Cancer Res 2006;12:6494–501.
16. Hochhaus A, Kantarjian HM, Baccarani M, et al. Dasatinib induces notable hematologic and cytogenetic responses in chronic-phase chronic myeloid leukemia after failure of imatinib therapy. Blood 2007;109:2303–9.
17. Shah NP, Tran C, Lee FY, Chen P, Norris D, Sawyers CL. Overriding imatinib resistance with a novel ABL kinase inhibitor. Science 2004;305:399–401.
18. Golemovic M, Verstovsek S, Giles F, et al. AMN107, a novel aminopyrimidine inhibitor of Bcr-Abl, has *in vitro* activity against imatinib-resistant chronic myeloid leukemia. Clin Cancer Res 2005;11:4941–7.
19. O'Hare T, Walters DK, Stoffregen EP, et al. *In vitro* activity of Bcr-Abl inhibitors AMN107 and BMS-354825 against clinically relevant imatinib-resistant Abl kinase domain mutants. Cancer Res 2005;65:4500–5.
20. Weisberg E, Manley PW, Breitenstein W, et al. Characterization of AMN107, a selective inhibitor of native and mutant Bcr-Abl. Cancer Cell 2005;7:129–41.
21. Demetri GD, van Oosterom AT, Garrett CR, et al. Efficacy and safety of sunitinib in patients with advanced gastrointestinal stromal tumour after failure of imatinib: a randomised controlled trial. Lancet 2006;368:1329–38.
22. Heinrich MC, Maki RG, Corless CL, et al. Sunitinib (SU) response in imatinib-resistant (IM-R) GIST correlates with KIT and PDGFRA mutation status. Proc Am Soc Clin Oncol Annu Meet 2006;24:9502.
23. Gendreau SB, Ventura R, Keast P, et al. Inhibition of the T790M gatekeeper mutant of the epidermal growth factor receptor by EXEL-7647. Clin Cancer Res 2007;13:3713–23.
24. de La Motte Rouge T, Galluzzi L, Olaussen KA, et al. A novel epidermal growth factor receptor inhibitor promotes apoptosis in non-small cell lung cancer cells resistant to erlotinib. Cancer Res 2007;67:6253–62.
25. Kwak EL, Sordella R, Bell DW, et al. Irreversible inhibitors of the EGF receptor may circumvent acquired resistance to gefitinib. Proc Natl Acad Sci U S A 2005;102:7665–70.
26. Cohen EE, Lingen MW, Martin LE, et al. Response of some head and neck cancers to epidermal growth factor receptor tyrosine kinase inhibitors may be linked to mutation of ERBB2 rather than EGFR. Clin Cancer Res 2005;11:8105–8.
27. Lee JW, Soung YH, Kim SY, et al. ERBB2 kinase domain mutation in the lung squamous cell carcinoma. Cancer Lett 2006;237:89–94.
28. Lee JW, Soung YH, Kim SY, et al. ERBB2 kinase domain mutation in a gastric cancer metastasis. APMIS 2005;113:683–7.
29. Lee JW, Soung YH, Seo SH, et al. Somatic mutations of ERBB2 kinase domain in gastric, colorectal, and breast carcinomas. Clin Cancer Res 2006;12:57–61.
30. Shigematsu H, Takahashi T, Nomura M, et al. Somatic mutations of the HER2 kinase domain in lung adenocarcinomas. Cancer Res 2005;65:1642–6.
31. Stephens P, Hunter C, Bignell G, et al. Lung cancer: intragenic ERBB2 kinase mutations in tumours. Nature 2004;431:525–6.
32. Wang SE, Narasanna A, Perez-Torres M, et al. HER2 kinase domain mutation results in constitutive phosphorylation and activation of HER2 and EGFR and resistance to EGFR tyrosine kinase inhibitors. Cancer Cell 2006;10:25–38.
33. Geyer CE, Forster J, Lindquist D, et al. Lapatinib plus capecitabine for HER2-positive advanced breast cancer. N Engl J Med 2006;355:2733–43.
34. Azam M, Latek RR, Daley GQ. Mechanisms of autoinhibition and STI-571/imatinib resistance revealed by mutagenesis of BCR-ABL. Cell 2003;112:831–43.
35. Xia W, Mullin RJ, Keith BR, et al. Anti-tumor activity of GW572016: a dual tyrosine kinase inhibitor blocks EGF activation of EGFR/erbB2 and downstream Erk1/2 and AKT pathways. Oncogene 2002;21:6255–63.
36. Stamos J, Sliwkowski MX, Eigenbrot C. Structure of the epidermal growth factor receptor kinase domain alone and in complex with a 4-anilinoquinazoline inhibitor. J Biol Chem 2002;277:46265–72.
37. Wood ER, Truesdale AT, McDonald OB, et al. A unique structure for epidermal growth factor receptor bound to GW572016 (lapatinib): relationships among protein conformation, inhibitor off-rate, and receptor activity in tumor cells. Cancer Res 2004;64:6652–9.
38. Zhang X, Gureasko J, Shen K, Cole PA, Kuriyan J. An allosteric mechanism for activation of the kinase domain of epidermal growth factor receptor. Cell 2006;125:1137–49.
39. Akiyama T, Matsuda S, Namba Y, Saito T, Toyoshima K, Yamamoto T. The transforming potential of the c-erbB-2 protein is regulated by its autophosphorylation at the carboxyl-terminal domain. Mol Cell Biol 1991;11:833–42.
40. Messerle K, Schlegel J, Hynes NE, Groner B. NIH/3T3 cells transformed with the activated erbB-2 oncogene can be phenotypically reverted by a kinase

deficient, dominant negative erbB-2 variant. Mol Cell Endocrinol 1994;105:1–10.

41. Piechocki MP, Yoo GH, Dibbley SK, Lonardo F. Breast cancer expressing the activated HER2/neu is sensitive to gefitinib *in vitro* and *in vivo* and acquires resistance through a novel point mutation in the HER2/neu. Cancer Res 2007;67:6825–43.

42. Carter TA, Wodicka LM, Shah NP, et al. Inhibition of drug-resistant mutants of ABL, KIT, and EGF receptor kinases. Proc Natl Acad Sci U S A 2005;102:11011–6.

43. Cools J, Mentens N, Furet P, et al. Prediction of resistance to small molecule FLT3 inhibitors: implications for molecularly targeted therapy of acute leukemia. Cancer Res 2004;64:6385–9.

44. Cameron D. Lapatinib plus capecitabine in patients with HER2-positive advanced breast cancer. Clin Adv Hematol Oncol 2007;5:456–8.

45. Vikis H, Sato M, James M, et al. EGFR-T790M is a rare lung cancer susceptibility allele with enhanced kinase activity. Cancer Res 2007;67:4665–70.

46. Godin-Heymann N, Bryant I, Rivera MN, et al. Oncogenic activity of epidermal growth factor receptor kinase mutant alleles is enhanced by the T790M drug resistance mutation. Cancer Res 2007;67:7319–26.

47. Xia W, Bacus S, Hegde P, et al. A model of acquired autoresistance to a potent ErbB2 tyrosine kinase inhibitor and a therapeutic strategy to prevent its onset in breast cancer. Proc Natl Acad Sci U S A 2006;103:7795–800.

48. Nagata Y, Lan KH, Zhou X, et al. PTEN activation contributes to tumor inhibition by trastuzumab, and loss of PTEN predicts trastuzumab resistance in patients. Cancer Cell 2004;6:117–27.

49. Mellinghoff IK, Cloughesy TF, Mischel PS. PTEN-mediated resistance to epidermal growth factor receptor kinase inhibitors. Clin Cancer Res 2007;13:378–81.

50. Yamasaki F, Johansen MJ, Zhang D, et al. Acquired resistance to erlotinib in A-431 epidermoid cancer cells requires down-regulation of MMAC1/PTEN and up-regulation of phosphorylated Akt. Cancer Res 2007;67:5779–88.

51. Kokubo Y, Gemma A, Noro R, et al. Reduction of PTEN protein and loss of epidermal growth factor receptor gene mutation in lung cancer with natural resistance to gefitinib (IRESSA). Br J Cancer 2005;92:1711–9.

52. Sergina NV, Rausch M, Wang D, et al. Escape from HER-family tyrosine kinase inhibitor therapy by the kinase-inactive HER3. Nature 2007;445:437–41.

53. Engelman JA, Zejnullahu K, Mitsudomi T, et al. MET amplification leads to gefitinib resistance in lung cancer by activating ERBB3 signaling. Science 2007;316:1039–43.

54. She QB, Solit D, Basso A, Moasser MM. Resistance to gefitinib in PTEN-null HER-overexpressing tumor cells can be overcome through restoration of PTEN function or pharmacologic modulation of constitutive phosphatidylinositol 3′-kinase/Akt pathway signaling. Clin Cancer Res 2003;9:4340–6.

55. Wang MY, Lu KV, Zhu S, et al. Mammalian target of rapamycin inhibition promotes response to epidermal growth factor receptor kinase inhibitors in PTEN-deficient and PTEN-intact glioblastoma cells. Cancer Res 2006;66:7864–69.